Powder Technology 415 (2023) 118141

Contents lists available at ScienceDirect

Powder Technology

journal homepage: www.journals.elsevier.com/powder-technology

On the friction/tangential restitution problem: Independent friction-restitution modeling of sphere rebound with arbitrary spin

Antonio Doménech-Carbó *

Department of Analytical Chemistry, University of Valencia, Dr. Moliner, 50, 46100 Burjassot, València, Spain

HIGHLIGHTS

- The concept of tangential coefficient of restitution is critically examined.
- Independent friction-restitution modeling is applied to sphere rebound with arbitrary spin.
- A unique set of coefficients of friction and restitution independent on the impact angle is used.
- The resulting modeling satisfactorily reproduces experimental data in recent oblique impact literature.

GRAPHICAL ABSTRACT

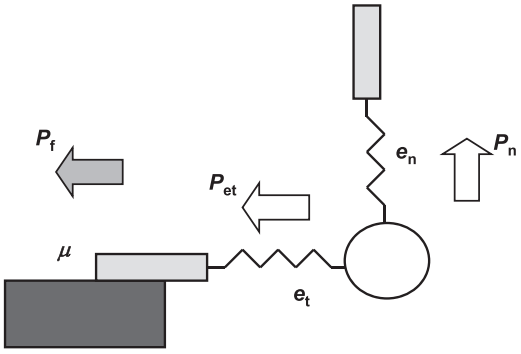

ARTICLE INFO

Keywords:
Collisions
Friction
Tangential and normal restitution
Stick
Slip

ABSTRACT

Most descriptions of collision events introduce coefficients of friction and tangential restitution which vary significantly with the impact angle, in contrast with the independence of the normal coefficient of restitution with this parameter. A redefinition of the coefficients of friction and tangential restitution based on the idea that friction and restitution effects can be treated as being mutually independent, provides a satisfactory description of experimental data using a 'constant' restitution coefficient independent on the impact angle. This independent friction-restitution modeling is developed here for the rebound of a homogeneous sphere having an arbitrary spin on a rough massive plane. The reported closure permits the interpretation of experimental data recently reported in literature.

1. Introduction

Along the last decades, the analysis of experimental data on planar collisions under moderate incoming velocities and in the absence of adhesive and viscous effects has been based on the models of Walton [1] and Maw et al. [2,3]. Both models are aimed to describe both the sticking and sliding regimes of impact and use the coefficient of tangential restitution, defined by analogy to the well-known coefficient of normal restitution and the coefficient of friction, based in the Amontons-Coulomb approach to friction [4,5].

The Walton's model implies a twofold asymmetry: by the first token, the tangential coefficient of restitution is taken as a constant in collisions

* Corresponding author.
E-mail address: antonio.domenech@uv.es.

https://doi.org/10.1016/j.powtec.2022.118141
Received 25 October 2022; Received in revised form 28 November 2022; Accepted 29 November 2022
Available online 5 December 2022

in stick regime while it varies with the impact angle for collisions in sliding regime. By the second token, the friction coefficient depends on the impact angle for collisions in sticking regime while it is taken as a constant in sliding regime. Experimental data on the rebound of spheres on massive planes have provided abundant evidence for the variation of the tangential coefficient of restitution [6–29] and the coefficient of friction (or its equivalent, the tangential to normal impulse ratio, vide infra) [7,8,14,24,26] with the angle of impact. Additionally, experimental data on non-planar collisions reveal that the tangential coefficient of restitution and the coefficient of friction defined in the Walton's model also varies with the rotation rate of the sphere [14,26,27]. These features are in sharp contrast with the normal coefficient of restitution, which remains essentially independent on the impact angle and the initial spin of the sphere within a wide range of experimental conditions in the majority of cases.

The above operational problem is accompanied by a conceptual one as far as, in principle, friction and restitution, can differently be conceived. The normal and tangential coefficients of restitution can be related with the mechanical properties of the materials (Young's modulus, Poisson's coefficient) via Hertz-type contact force models [30–37]. Although these models predict a variation of the normal coefficient of restitution with the incoming velocity of the colliding bodies, this variation can be neglected under most 'ordinary' conditions. On the contrary, the friction impulses can be seen as depending on surface properties such as asperity, roughness, etc. [30]. Then, although both influencing the impact dynamics, restitution and friction can be viewed as separate mechanisms operating separately, as expressed in spring-damping contact models [33,37].

In this context, it was formulated a different theoretical closure based on the idea that friction and restitution operate conjointly but independently through the impact [38,39]. The model defines the coefficients of restitution (friction) in terms of the normal and tangential velocities of the contact point in the absence of friction (in the absence of restitution) effects. These idealized definitions permit to obtain a series of dynamic equations in agreement with experimental data using restitution coefficients independent on the incidence angle. This formulation permitted the interpretation of a series of experimental data considered as 'anomalous' in literature [7,8,12,14,16], as becoming within the 'ordinary' impact behavior described by the so-called independent friction-restitution (IFR) model. Successive refinements on friction effects were subsequently reported [40–43] allowing for the interpretation of new experimental details on the rebound of macrospheres [7,9,11,14] and microspheres [6,10,15,19,20,24] on massive half-planes.

The proposed IFR model, as the Walton's one, uses the phenomenological coefficients of restitution and friction which can be determined from experimental data obtained during the impact event. This is a difference with the Maw et al. model [2,3], which was formulated in terms of the Young's modulus and Poisson's coefficients of the colliding bodies, needing to be known, as emphasized by Kim and Dunn [15], independently from the experimental data recorded in the impact event.

The purpose of the current work is: a) to analyze with some detail the conceptual and operational problems associated to the view of the coefficient of tangential restitution in the aforementioned friction-restitution (in the following FR) models; b) provide a general IFR formulation of the rebound of a homogeneous sphere on a rough, massive plane when an arbitrary spin has been imparted to the sphere; c) analyze experimental data in recent literature [23–29] which has not been previously examined under the IFR modeling. As a result, it is concluded that, based on the IFR redefinition of tangential coefficient of restitution, new experimental data can also be satisfactorily interpreted using 'constant' tangential restitution coefficients.

2. Theory

2.1. General approach

Let us consider the planar oblique impact of a homogeneous sphere of mass m, radius R, and inertia moment I (= (2/5)mR^2) on an infinitely massive, rough wall, as schematized in Fig. 1. It will be assumed that there is contact through a single point of the sphere without significant deformation. Let **u** and **v** the pre-impact and post-impact center of mass velocities and **U**, **V**, the respective velocities of the contact point.

The general description of the impact dynamics is based on the Newton's laws for linear and angular impulses. These can be expressed here on saying that the total impulse (i.e., the sum of individual impulses due to different factors) acting on the sphere will determine the change in its center of mass velocity and the total angular impulse the change in the rotation rates. To complete the description of the impact event, however, constitutive definitions of the individual forces/impulses (i.e., those due to friction, restitution, or even other possible factors) are needed. Accordingly, the normal and tangential center of mass velocities (denoted in the following by the subscripts n, t) will change under the action of normal and tangential impulses, $\mathbf{P_n}$, $\mathbf{P_t}$, as,

$$P_n = m(v_n - u_n) \tag{1}$$

$$P_t = m(v_t - u_t) \tag{2}$$

It will be assumed that the center of mass velocity is directed along the x-axis and that, as schematized in Fig. 1, arbitrary spins ω_x, ω_y, ω_z, have been imparted to the sphere before the impact. Accordingly, the prerebound velocity of the contact point will have three components:

$$U_x = usin\gamma + R\omega_y; \quad U_y = R\omega_x; \quad U_z = ucos\gamma \tag{3}$$

The angular velocities, Ω_x, Ω_y, Ω_z, after the impact can be derived from the classical law of angular impulse: the net angular impulses acting on the sphere in the x, y, and z directions will equal the product of the inertia moment of the sphere by the change in the corresponding angular velocities. Taking $I = (2/5)mR^2$, this law yields,

$$R\Omega_x = \frac{5}{2}\frac{P_{ty}}{m}; \quad R\Omega_y = \frac{5}{2}\frac{P_{tx}}{m}; \quad \Omega_z = \omega_z \tag{4}$$

where P_{tx}, P_{ty} represent the x- and y-components of the tangential impulse. The contact point velocities, V_x, V_y, V_z, satisfy the relationships $V_x = v_x + R\Omega_y$; $V_y = v_y + R\Omega_x$; $V_z = v_z$.

The normal coefficient of restitution can be defined in several ways [4,5]. Here, the canonical kinematic definition in terms of the normal components of the contact point velocity will be used:

$$e_n = -\frac{V_n}{U_n} \tag{5}$$

Then, the normal impulse will be:

$$P_{en} = -m(1+e_n)U_n = -m(1+e_n)ucos\gamma \tag{6}$$

2.2. Friction & restitution modeling

To complete the dynamic study, there is need of defining constitutive impulse functions [34–36]. This is the crucial point where the proposed models differ. For our purposes, the relevant point to emphasize is that there are no restrictions to be imposed a priori to the different forces/impulses; the unique condition is that their sum satisfies the aforementioned Newton's laws. Accordingly, i) it is possible to independently define impulses due to restitution and friction; ii) these impulses can freely be associated to different impact parameters such as the center of mass and/or the contact point velocities. This arbitrary definitional character is reflected in the fact that different definitions of the tangential coefficient of restitution are used in literature, including kinematic, dynamic, and energetic [5], and kinematic definitions in terms

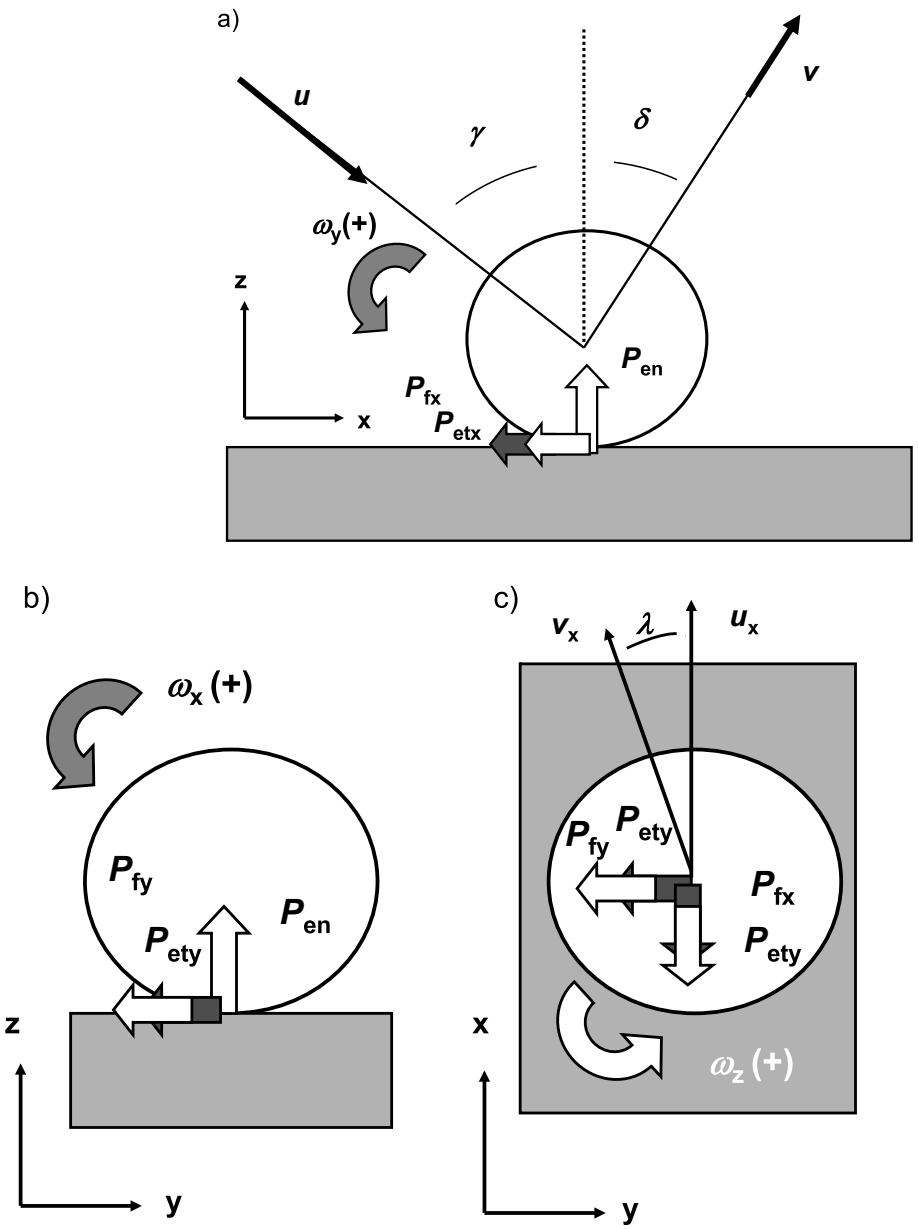

Fig. 1. Schemes of the oblique impact of a homogeneous sphere on an infinitely massive rough plane for the case of arbitrary initial spins. a) Lateral view along the *y*-axis; b) view along the *x*-axis; c) zenithal view (along the *z*-axis).

of contact point and center of mass velocities [14,17,23,24].

For simplicity, we will present here the results for planar rebounds; i.e., when the pre- and postrebound linear velocity vectors are all placed within a common plane. This implies that, according to the scheme in Fig. 1, the tangential direction is coincident with the *x*-axis (i.e., that the subscripts x and t have identical meaning). This not will be valid for non-planar collisions which will be treated in the next section for the IFR model. In the first model accounting for the discrimination between stick and slip collisions, due to Brach [4,44], it was assumed that in sliding regime, the tangential impulse was the coefficient of friction (μ) times the normal impulse, i.e.,

$$P_x = \pm \mu m(1+e_n)ucos\gamma \tag{7}$$

while the condition of stick regime was $V_t = 0$. This implies that $v_x + R\Omega_y = 0$. Since Eqs. (1)–(4) permit to write: $v_x = u_x + P_x/m$ and $R\Omega_y = R\omega_y + (5/2)P_x/m$, the above condition implies that the tangential impulse equals to,

$$P_x = \pm \frac{2}{7} m(usin\gamma + R\omega_y) \tag{8}$$

It is pertinent to note that the direction of the tangential impulse is that opposite to the direction of U_t; i.e., the tangential component of the velocity of the contact point before the impact. For simplicity, the case where $v_x + R\omega > 0$ will be considered in the following.

Notice that the above model applies to tangential impulses the well-known formalism of Amontons-Coulomb friction: in sliding regime the tangential impulse is μ times the normal impulse and in sticking regime the tangential impulse equals that necessary to maintain the surfaces in contact relatively at rest. This friction-based model (F-model), however, cannot entirely explain the postrebound velocities appearing in stick regime, where in general $V_t \neq 0$. The Walton's model attempted to reproduce these experimental features [1] assuming that restitution effects also operate in the tangential direction. Here, in collisions with sticking, the tangential impulse was expressed in terms of the coefficient of tangential restitution, defined by analogy to the coefficient of normal

restitution as,

$$\beta = -\frac{V_t}{U_t} = -\frac{V_x}{U_x} \tag{9}$$

In several cases, β is defined with the opposite sign and, in others, replacing the contact point by the center of mass velocities [14,17,23,24]. Using the definition in Eq. (9), that the tangential impulse is,

$$P_x = -\frac{2}{7}(1+\beta)mU_t = -\frac{2}{7}(1+\beta)m(usin\gamma + R\omega_y) \tag{10}$$

In turn, when the collision takes place in sliding regime, Eq. (7) applies, thus defining a friction-restitution (FR) closure. For brevity, the expressions for the postimpact linear and angular velocities are listed in the Appendix A1. Remarkably, in sticking regime the FR coefficient of tangential restitution possesses a constant value β, while in sliding regime it varies significantly with the impact angle, being related to the coefficient of sliding friction by the relationship,

$$\beta = \frac{7}{2}\mu(1+e_n)\left(\frac{cos\gamma}{sin\gamma + R\omega_y/u}\right) - 1 \tag{11}$$

i.e., the as-defined coefficient of tangential restitution can be expressed as a function of the impact angle and the coefficient of sliding friction. For the case of rebound without initial spin, and assuming that μ is constant, Eq. (11), predicts a linear variation of β with cotanγ. The FR model reduces to the F one taking $\beta = 0$ and can be interpreted, as far as $V_t \neq 0$, as implying that the coefficient of friction varies with the impact angle in sticking regime. Strictly, the friction coefficient can only be defined in sliding regime as the tangential impulse to normal impulse ratio (in absolute value), i.e., $\mu = |P_t|/|P_n|$. If this is extended to the sticking regime, friction coefficients depending on the impact angle are obtained (for instance, in [26]). The measurement of the coefficient of sliding friction in impact events has to be made, however, from the directly measured quantities, usually the center of mass velocities. Then, operationally, μ is defined/measured in planar impacts as the absolute value of the $(v_x\text{-}u_x)/(v_z\text{-}u_z)$ ratio. Under this view of the Walton's model, the coefficient of sliding friction will be equal toμ, regardless the incident angle value in sliding regime but, in sticking regime, it will vary with the impact angle according to,

$$\mu = \frac{|v_x - u_x|}{|v_z - u_z|} = \frac{2}{7}\left(\frac{1+\beta}{1+e_n}\right)\left(tan\gamma + \frac{R\omega_y}{ucos\gamma}\right) \tag{12}$$

As will be discussed below, in the IFR model this definition, as incorporates both friction and tangential restitution effects, yields an 'apparent' coefficient of friction.

2.3. Conceptual and operational problems

The above modeling provides a satisfactory agreement with experimental data except in several 'anomalous' cases [7,8,12,14,16]. However, this treatment involves several conceptual problems. As previously noted, the model leads to an intriguing situation condensed in Eqs. (11) amd (12): i) the tangential coefficient of restitution is constant in sticking regime while varies with the impact angle in sliding regime, and ii) the coefficient of friction is constant in sliding regime while depends on the impact angle in sticking regime. These variations abruptly contrasts with the constancy assumed for the coefficient of normal restitution in both sticking and sliding regimes of impact. In fact, experimental data reveal that β values exhibit gross changes with the impact angle for collisions in sliding regime [8,9,14,16,19–29] and, when impact with initial spin is studied [14,26,27], with the initial rotation rate, both in contrast with the constancy of e_n in the same set of experiments. Similarly, the friction coefficient (or its equivalent tangential to normal impulse ratio) significantly varies with the impact angle in collisions in sticking regime [7,8,14,24,26]. This leads to a first conceptual problem: since in principle friction and restitution are mechanisms influencing the dynamics of impact events, how they behave so differently when sticking and sliding regimes are considered?

The second problem is more subtle. De facto, friction and restitution are seen as different physical mechanisms acting throughout the impact [4,5] at least at the so-called mesoscopic scale [28]. At this scale, friction depends on the surface properties (asperities, roughness) whereas restitution should be dependent on the 'elastic' properties (Young's modulus, Poisson's coefficient) of the bulk of the material. In fact, much literature emphasizes the difference between these mechanisms on describing impact in terms of spring plus dashpot assemblies [33,37] (see, for instance, Fig. A1 in ref. [33]), as schematized in Fig. 2.

In this context, one possible operational view of the Walton's FR model is that tangential restitution operates solely in the sticking regime whereas friction operates in the sliding regime. The question around this view is: why each one of the mechanisms operates in one of the two possible impact regimes? A second interpretation of the FR closure is that friction and restitution, although conceptually different, cannot be separately treated. This second view is also problematic, as can be discussed around the interpretation of Eqs. (11) and (12). In principle, these equations mean not only that the restitution and friction mechanisms are directly related, but also that they are equivalent (but with different equivalence relationships in sticking and sliding regimes). If this view is adopted, why is the reason for this equivalence?, why tangential restitution (and friction) changes so drastically its behavior from sticking to sliding conditions? As described in the next section, these questions can be treated differently by adopting a new definition of the tangential restitution coefficient just expressing the conceptual difference between friction and tangential restitution.

2.4. IFR modeling

The IFR model assumes that the impulses due to friction and restitution act independently throughout the impact. Now, let us consider the general case in which a homogeneous sphere rebounds on an infinitely massive plane with arbitrary rotation rates. It will be assumed that the center of mass initial velocity is directed along the x-axis and that the normal impulse is directed in the z-direction. This can be expressed as:

$$\mathrm{P_{en}\cdot n} = -m(1+e_n)(\mathrm{U\cdot n})sign[\mathrm{U\cdot n}] \tag{13}$$

Here, sign [] represents the sign function [12,35] and **n** the unit vector in the normal direction. In the IFR closure, the tangential coefficient of restitution, e_t, is redefined as the negative ratio of the postimpact to preimpact tangential velocities of the contact point *in the absence of frictional effects*, V^*_t, U^*_t, as [38,39],

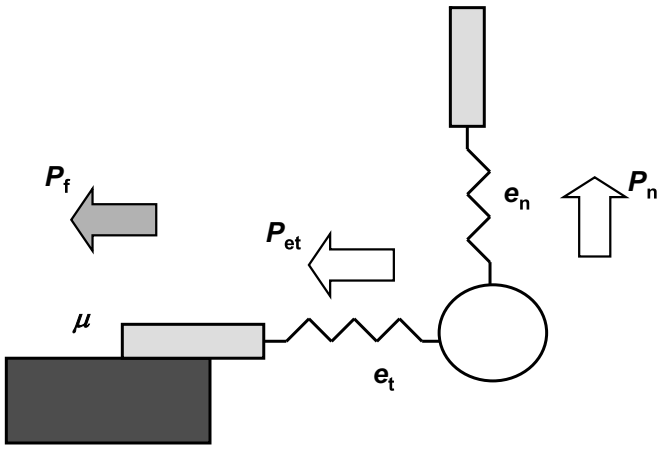

Fig. 2. Schematics of the spring plus dashpot representation used to describe impact dynamics.

$$e_t = -\frac{V_t^*}{U_t^*} \tag{14}$$

Then, the tangential impulse due to tangential restitution, P_{et}, can be expressed as,

$$P_{et}\cdot t = -\frac{2}{7}m(1+e_t)(U\cdot t)sign[U\cdot t] \tag{15}$$

where **t** is the unit vector in the tangential direction. The net tangential impulse will be the sum of P_{et} with the impulse due to friction, P_f. Following the Amontons-Coulomb view of friction, it will be assumed that, when the impact occurs in sliding regime, the frictional impulse will be μ times the normal impulse. This means that the friction coefficient is defined as the tangential to normal impulse ratio *in the absence of tangential restitution effects* [38,39]. Then,

$$P_f\cdot t = -\mu m(1+e_t)(U\cdot n)sign[U\cdot t] \tag{16}$$

Following the same view of friction, the friction impulse operating in sticking regime will be approximated by the percussion center approach [40] as,

$$P_f\cdot t = -\frac{2}{5}m(U\cdot t)sign[U\cdot t] \tag{17}$$

Assuming, as before, that there are no significant effects of rolling and pivoting friction, the above impulses can be rewritten in function of the angle of lateral deviation at the contact point, σ, defined as,

$$tan\sigma = \frac{R\omega_x}{usin\gamma + R\omega_y} = \frac{R\omega_x/u}{sin\gamma + R\omega_y/u} \tag{18}$$

This angle is representative of the direction of the contact point initial velocity vector in the *xy* plane, U_{xy}, whose absolute value is,

$$U_{xy} = \sqrt{\left(usin\gamma + R\omega_y\right)^2 + \left(R\omega_x\right)^2} = u\sqrt{\left(sin\gamma + R\omega_y/u\right)^2 + \left(R\omega_x/u\right)^2} \tag{19}$$

where, as in Eq. (18), the non-dimensional coefficients $R\omega_x/u$ and $R\omega_y/u$ have being introduced. Accordingly, the normal impulse is again given by Eq. (6) and the tangential impulse due to restitution can be separated into *x*- and *y*-components (P_{ex}, P_{ey}) given by the expressions,

$$P_{ex} = -\frac{2}{7}m(1+e_t)U_{xy}cos\sigma; \quad P_{ey} = -\frac{2}{7}m(1+e_t)U_{xy}sin\sigma \tag{20}$$

In turn, the frictional impulses acting in sliding and sticking regimes in the *x*- and *y*-direction are, respectively,

$$P_{fx} = \mu m(1+e_n)ucos\gamma cos\sigma; \quad P_{fy} = \mu m(1+e_n)ucos\gamma sin\sigma \tag{21}$$

$$P_{fx} = \frac{2}{5}mU_{xy}cos\sigma; \quad P_{fy} = \frac{2}{5}mU_{xy}sin\sigma \tag{22}$$

The corresponding expressions for the postcollision linear and angular velocities are shown in the Appendix A1. These equations reduce to those previously reported [40] for planar impacts taking $\sigma = 0$. In the case of sliding impacts, the same equations reduce to the FR model taking $e_t = -1$. An interesting particular case is obtained when the normal coefficient of restitution becomes zero. In this case, the center of mass rebound velocity in the *z*-direction becomes zero and the sphere will move along the massive plane (i.e., the rebound angle $\delta = 0$). However, assuming that the coefficients of tangential restitution and friction are independent on e_n, the postrebound velocities in the *x*- and y-directions will not be zero and will be dependent on the incidence angle (see Appendix A1).

The transition between the sticking and sliding regimes takes place at an impact angle γ_T satisfying the relationship,

$$cos\gamma_T = \frac{2}{5}\left(\frac{U_{xy}}{u}\right)\left(\frac{1}{\mu(1+e_n)}\right) \tag{23}$$

For the case of planar impacts without initial spin, the above equation reduces to,

$$tan\gamma_T = \frac{5}{2}\mu(1+e_n) \tag{24}$$

2.5. Tangential coefficients of restitution

The restitution coefficient defined in the FR closure, β, is now given by,

$$\beta = -\frac{\sqrt{V_x^2 + V_y^2}}{\sqrt{\left(usin\gamma + R\omega_y\right)^2 + \left(R\omega_x\right)^2}} \tag{25}$$

This 'apparent' FR tangential coefficient of restitution will be dependent on the impact angle and the initial rotation rates. It can be expressed as a function of the 'constant' coefficient of tangential restitution defined in the IFR formalism, e_t, from the velocity expressions in the Appendix A1. In the simplest case of planar impacts eq. (25) reduces to, for collisions in sliding regime:

$$\beta = e_t + \frac{7}{2}\mu(1+e_n)\left(\frac{cos\gamma}{sin\gamma + R\omega_y/u}\right) \tag{26}$$

This equation reduces to the FR Eq. (11) taking, as previously noted, $\omega_y = 0$, and $e_t = -1$. For collisions in sticking regime,

$$\beta = \left(\frac{7}{5} + e_t\right) \tag{27}$$

Eq. (26) means that the variation of the FR tangential coefficient of restitution (β) on the impact angle observed in sliding regime can be re-interpreted as 'apparent', the 'true' tangential coefficient of restitution (e_t) being constant.

The tangential coefficient of restitution referred to the center of mass velocities, β_{CM} ($\beta_{CM} = -(v_t/u_t)$), used by several authors [14,17,23,24], can also be obtained for planar collisions as,

$$\text{Sticking regime}: \beta_{CM} = \left[\frac{2}{7}(1+e_t) + \frac{2}{5}\right]\left(1 + \frac{R\omega_y}{usin\gamma}\right) - 1 \tag{28}$$

$$\text{Sliding regime}: \beta_{CM} = \frac{2}{7}(1+e_t)\left(1 + \frac{R\omega_y}{usin\gamma}\right) + \mu(1+e_n)\text{cotan}\gamma - 1 \tag{29}$$

These authors combine the tangential and normal coefficients of restitution to define a total (center of mass) coefficient of restitution, β_{tot}, as $\beta_{tot} = [(e_n\cos\gamma)^2 + (\beta\sin\gamma)^2]^{1/2}$.

2.6. Friction coefficients

Experimental data on collisions are unanimously taken from velocity measurements using different devices [6–29]. As briefly discussed in the section 2.1, the 'apparent' coefficient of friction defined in the FR closure [12,26] will be calculated as the ratio $(v_x\text{-}u_x)/(v_z\text{-}u_z)$ which is equivalent to the P_{tx}/P_n tangential to normal impulse ratio. In the IFR modeling, the expressions for planar collisions in sliding and sticking regimes are,

$$\mu_{app} = \mu + \frac{2}{7}\left(\frac{1+e_t}{1+e_n}\right)\left(tan\gamma + \frac{R\omega_y}{ucos\gamma}\right) \tag{30}$$

$$\mu_{app} = \left[\frac{\frac{2}{7}(1+e_t) + \frac{2}{5}}{1+e_n}\right]\left(tan\gamma + \frac{R\omega_y}{ucos\gamma}\right) \tag{31}$$

respectively.

2.7. Rebound angles

The general expressions for rebound angle in the *xz* plane (see Fig. 1a) will be, for collisions in sticking regime,

$$tan\delta = \frac{1}{e_n}tan\gamma - \frac{1}{e_n}\left[\frac{2}{5}+\frac{2}{7}(1+e_t)\right]\left(\frac{U_{xy}}{u}\right)\left(\frac{cos\sigma}{cos\gamma}\right) \quad (32)$$

and, for collisions in sliding regime,

$$tan\delta = \frac{1}{e_n}tan\gamma - \frac{2}{7}\left(\frac{1+e_t}{e_n}\right)\left(\frac{U_{xy}}{u}\right)\left(\frac{cos\sigma}{cos\gamma}\right) - \mu\left(\frac{1+e_n}{e_n}\right)cos\sigma \quad (33)$$

These equations become notably simplified for planar collisions ($\omega_x = 0$). If $\omega_x \neq 0$, there will be a lateral deviation of the sphere after the impact as schematized in Fig. 1c. The angle of deviation,λ, will be given, for rebounds in sticking and sliding regimes, by the relationships,

$$tan\lambda = \frac{\left[\frac{2}{5}+\frac{2}{7}(1+e_t)\right]\left(\frac{U_{xy}}{u}\right)sin\sigma}{sin\gamma - \left[\frac{2}{5}+\frac{2}{7}(1+e_t)\right]\left(\frac{U_{xy}}{u}\right)cos\sigma} \quad (34)$$

$$tan\lambda = \frac{-\frac{2}{7}(1+e_t)\left(\frac{U_{xy}}{u}\right)sin\sigma - \mu(1+e_n)cos\gamma sin\sigma}{sin\gamma - \frac{2}{7}(1+e_t)\left(\frac{U_{xy}}{u}\right)cos\sigma - \mu(1+e_n)cos\gamma cos\sigma} \quad (35)$$

respectively. For testing experimental data, it is frequent to use the representation of the impact angle at the contact point after the impact, ψ_{after}, vs. that angle just before the impact, ψ_{before}. In the case of planar collisions, $tan\psi_{after} = V_x/U_z$, and $tan\psi_{before} = U_x/U_z$, and the corresponding expressions for rebounds without initial spin are,

$$\text{Sticking regime}: tan\psi_{after} = -\left(\frac{7}{5}+e_t\right)tan\psi_{before} \quad (36)$$

$$\text{Sliding regime}: tan\psi_{after} = -e_t tan\psi_{before} - \frac{7}{2}\mu(1+e_n) \quad (37)$$

3. Comparison with experimental data

3.1. Tangential coefficient of restitution

Fig. 3 shows the variation of the FR tangential restitution coefficient with the incidence angle for collisions of a 20 mm diameter steel ball obliquely projected without initial spin on a polished granite block reported by Cross [26]. In this figure, the experimental data are superimposed to the theoretical lines from Eqs. (26) (sticking regime) and (27) (sliding regime) taking $\omega_y = 0$ and the values of e_n (0.94) and μ. (0.12) calculated by this author and $e_t = -0.98$. One can see that, despite relatively large dispersion in experimental data, the theoretical IFR lines satisfactorily reproduce the experimental results.

Similar agreement between experimental data and theoretical expectances was obtained for the oblique impact of γ-Al_2O_3 granules of 1.74 mm diameter on a glass plate target reported by Buck et al. [23]. Experimental data in Fig. 4a can be fitted to Eq. (27) taking $e_n = 0.78$, $e_t = -0.80$, and $\mu = 0.01$. Experimental data for the collisions of a 20 mm diameter steel ball impacting a steel plate reported by Hashemnia and Askari [27] can also be fitted to Eq. (27) taking $e_n = 0.60$, $e_t = -0.75$, and $\mu = 0.15$ (notice the definition of β and β_{CM} in literature differing by a minus sign from those used here). The agreement between these data and the theoretical curve can be seen in Fig. 4b, where -β is plotted vs. the ratio U_t/U_n (= tanγ).

Fig. 5 depicts the experimental β_{tot} data reported by Reagle et al. [21] for the planar ($\omega_x = 0$) collisions of Arizona road dust of 20–40 μm diameter on polished SAE 304 stainless steel at 27 m s^{-1} and reproduced

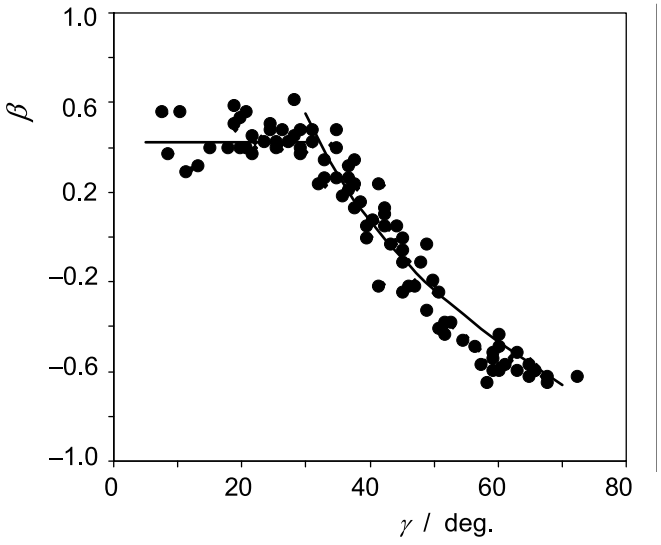

Fig. 3. Dependence of β on the impact angle at this for planar oblique collisions of 20 mm diameter steel ball projected without initial spin on a polished granite block reported by Cross [26]. Continuous lines correspond to theoretical predictions using Eqs. (26) (sticking regime) and (27) (sliding regime) taking $\omega_y = 0$, $e_n = 0.94$, $e_t = -0.98$, μ. = 0.12.

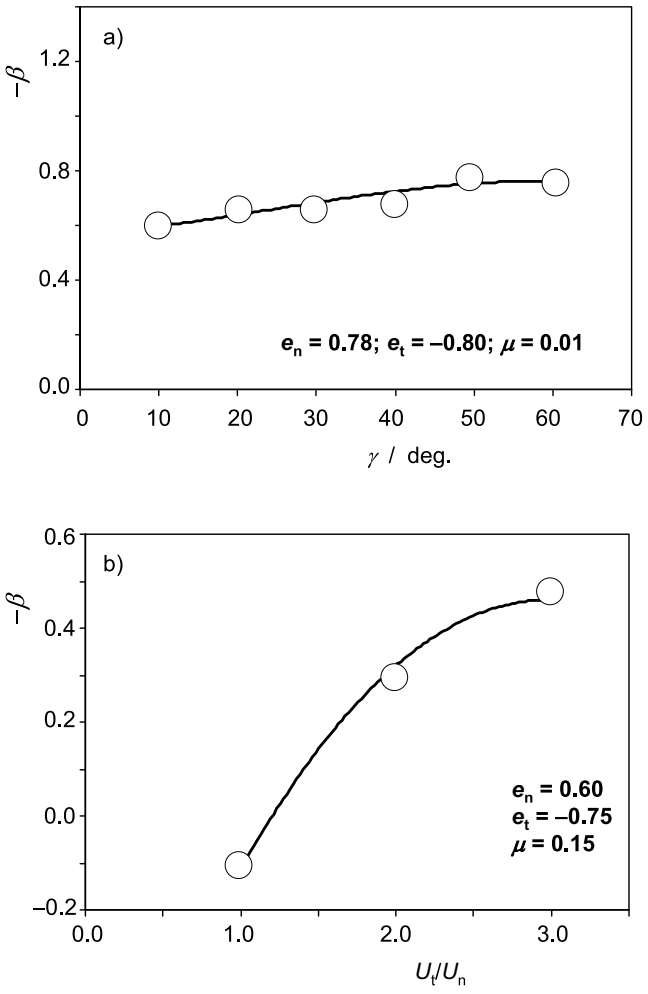

Fig. 4. a) Dependence of -β on: a) the impact angle for γ-Al_2O_3 granules of 1.74 mm diameter on a glass plate reported by Buck et al. [23], and, b) the ratio U_t/U_n (= tanγ) incidence angle for oblique collisions of 20 mm diameter steel ball projected without initial spin on a steel plate reported by Hashemnia and Askari [27]. Continuous lines correspond to theoretical predictions using Eq. (27) (sliding regime) taking $\omega_y = 0$ and the values of the coefficients of friction and restitution indicated in the graphs.

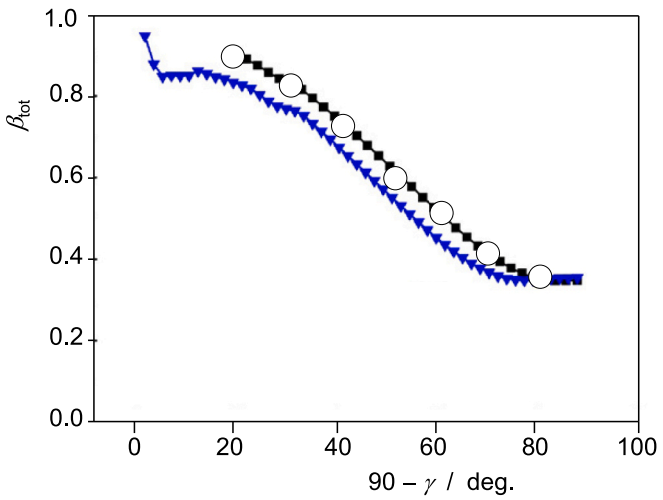

Fig. 5. Variation of β_{tot} on the impact angle reported by Reagle et al. [21] for the collisions of Arizona road dust of 20–40 μm diameter on polished SAE 304 stainless steel at 27 m s^{-1}, (solid squares) and theoretical expectances from the model of Yu and Tafti [22] (solid triangles). The circles correspond to the theoretical points calculated from Eqs. (28) and (29) taking $\omega_y = 0$, $e_n = 0.38$, $e_t = -0.95$ and $\mu = 0.10$.

by Yu and Tafti [22]. The experimental data are superimposed to the theoretical ones calculated by these authors (see ref. [22] for details) and the IFR model using Eqs. (28) and (29) taking $\omega_y = 0$, $e_n = 0.38$, $e_t = -0.95$ and $\mu = 0.10$. One can see here that the IFR closure can also satisfactorily reproduce experimental data when center of mass restitution coefficients are used.

The IFR model also applies satisfactorily for sphere rebounds with initial spin. In Fig. 6, the β vs. γ plots using experimental data for the rebound of a steel ball on a polished granite block with different initial spins in ref. [26], are depicted. In these experiments, a 20 mm diameter steel ball was projected with linear velocity of 2.0 ± 0.5 m s^{-1} and rotation rate of 45 ± 15 rad s^{-1} (circles), and linear velocity of 1.5 ± 0.6 m s^{-1} and rotation rate of 125 ± 25 rad s^{-1} (slid circles), respectively. In

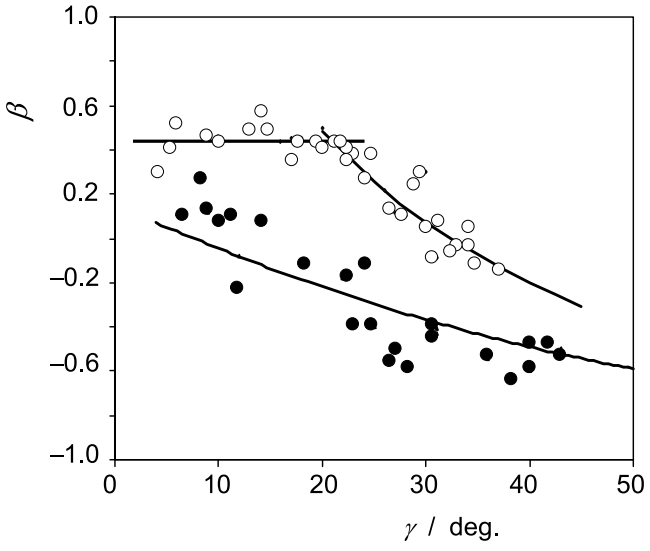

Fig. 6. Plots of β vs. the incidence angle for oblique collisions of 20 mm diameter steel ball projected on a polished granite block reported by Cross [26]. Circles: linear velocity 2.0 ± 0.5 m s^{-1}, rotation rate 45 ± 15 rad s^{-1}; solid circles: linear velocity 1.5 ± 0.6 m s^{-1}, rotation rate 125 ± 25 rad s^{-1}. Continuous lines correspond to theoretical lines inserting $e_n = 0.94$, $e_t = -0.98$, $\mu. = 0.14$ into Eqs. (26) (sticking regime) and (27) (sliding regime) and $R\omega_y/u = 0.225$ (circles) and $R\omega_y/u = 0.833$ (solid circles), respectively.

the first case, $R\omega_y/u = 0.225$, the sticking and sliding regimes take place depending on the impact angle whereas in the second, $R\omega_y/u = 0.833$, and only the sliding regime was attained. Both sets of data can satisfactorily be reproduced by theoretical lines from Eqs. (26) (sticking regime) and (27) (sliding regime) inserting the same set of values of the friction and restitution coefficients: $e_n = 0.94$, $e_t = -0.98$, $\mu. = 0.14$.

3.2. Rebound angles and apparent friction coefficients

Fig. 7 illustrates the variation of the rebound angle on the impact angle for planar oblique collisions without initial spin of spherical glass particles of diameter 165 μm on polished steel surface reported by Wang et al. [28]. Here, the impact velocity ranged between 5.9 m s^{-1} and 6.1 m s^{-1}. The reported experimental data can be reproduced using Eq. (33) (sliding regime) taking $e_n = 0.80$, $e_t = -0.98$, $\mu. = 0.11$.

Plots of rebound angle at the contact point vs. the impact angle at this point for planar oblique collisions of 20 mm diameter steel ball projected without initial spin on a polished granite block [26] are depicted in Fig. 8. Experimental data can satisfactorily be fitted to Eqs. (36) (sticking regime) and (37) (sliding regime) taking $e_n = 0.94$, $e_t = -0.98$, $\mu. = 0.12$. Similar agreement was obtained for the variation of the apparent coefficient of friction with the impact angle corresponding to the same set of experiments [26]. In this figure, experimental data points are superimposed in the sticking region to the theoretical line from Eq. (30) taking $e_n = 0.94$ and $e_t = -0.98$. In the sliding region, the prediction of the FR model (dotted line, $e_t = -1$) is accompanied by the theoretical lines from Eq. (31) taking $e_n = 0.94$, $\mu. = 0.12$, and four different values of e_t. One can see in this figure that, despite relatively high data dispersion in the sliding regime, experimental points diverge from the expectance from the FR model. This is just the 'anomalous' result underlined in literature [7,8,12,14,16].

The 'apparent' variation of the coefficient of friction with the impact angle is illustrated in Fig. 9, where experimental data for oblique collisions of a steel ball colliding on a projected granite block reported by Cross [26] are superimposed in the sticking region (low impact angles) to the theoretical line from Eq. (30) taking $e_n = 0.94$, $e_t = -0.98$. In the sliding region (high impact angles) several theoretical lines calculated

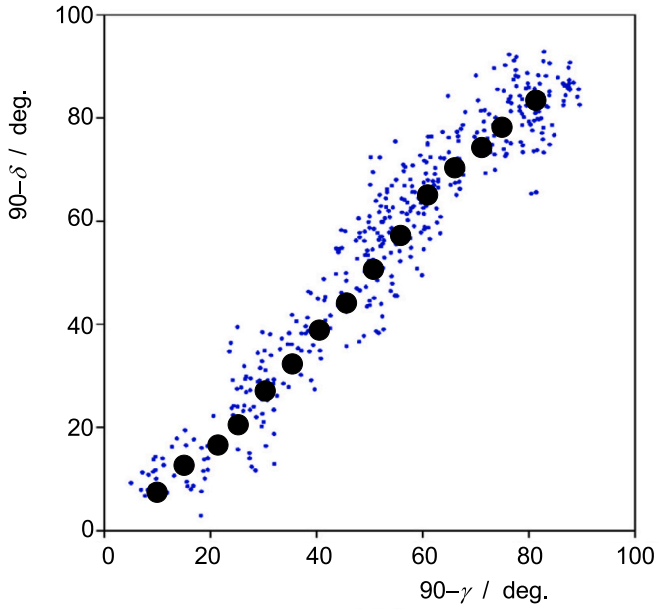

Fig. 7. Dependence of the rebound angle on the impact angle for planar oblique collisions without initial spin of spherical glass particles (diameter 165 μm) on polished steel wall with impact velocity between 5.9 m s^{-1} and 6.1 m s^{-1} reported by Wang et al. [28]. The gross points correspond to theoretical predictions using Eqs. (32) (sticking regime) and (33) (sliding regime) taking $e_n = 0.80$, $e_t = -0.98$, $\mu. = 0.11$.

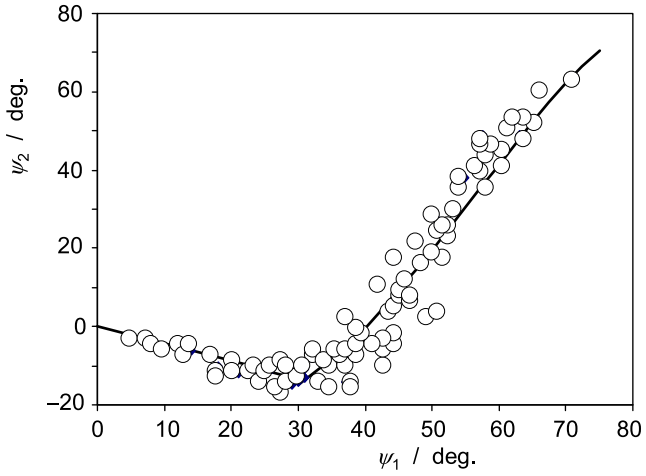

Fig. 8. Plots of rebound angle at the contact point vs. the impact angle at this for planar oblique collisions of 20 mm diameter steel ball projected without initial spin on a polished granite block reported by Cross [26]. Continuous lines correspond to theoretical predictions using Eqs. (36) (sticking regime) and (37) (sliding regime) taking $e_n = 0.94$, $e_t = -0.98$, $\mu. = 0.12$.

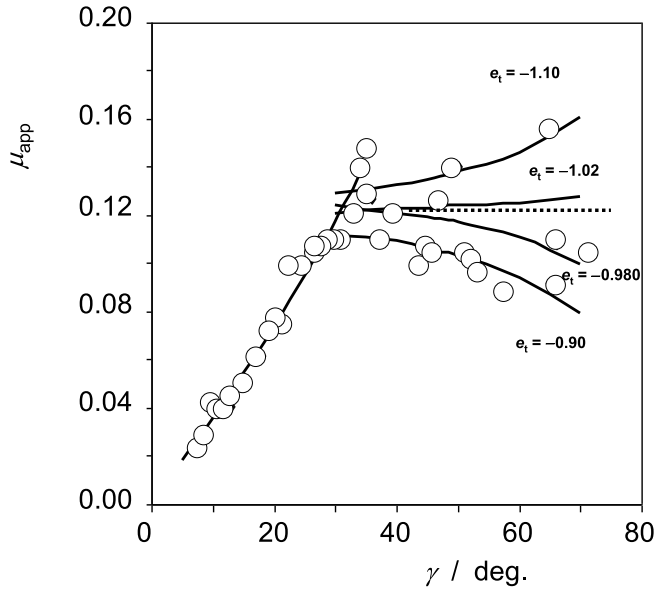

Fig. 9. Variation of the apparent friction coefficient on tanγ for oblique collisions of 20 mm diameter steel ball projected without initial spin on a polished granite block reported by Cross [26]. Continuous lines: theoretical line from Eq. (30) (sticking regime) taking $e_n = 0.94$, $e_t = -0.98$ and lines from Eq. (31) (sliding regime) taking $e_n = 0.94$, $\mu. = 0.12$, and four different values of e_t. The dotted line corresponds to $e_t = -1$, just the prediction of the FR model.

from Eq. (31) taking $e_n = 0.94$, $\mu. = 0.12$, and different values of e_t are depicted. The conventional FR model corresponds to $e_t = -1$.

Experimental results on collisions are frequently characterized by relatively high levels of data dispersion [28]. This scattering has been attributed to particle material properties and minor imperfections or local inhomogeneities of the surfaces [45]. This is illustrated in Fig. 9, where one can see that minute changes in the e_t value determine significant changes in the 'apparent' friction coefficient. A variety of factors can be responsible, including fluctuations in the direction and incoming velocity of the colliding bodies in replicate experiments. An additional factor to be considered is the possibility of (either randomized or biased) unexpected rotation rates. Although with except of few examples, experimental data on rebounds are carried out projecting the sphere without initial spin, there is possibility that, depending on the characteristics of the dropping or launching device, some initial angular velocities appear. Although there is no disposal of experimental data on rebounds with $\omega_x \neq 0$ where lateral deviation occurs (i.e., $\lambda \neq 0$), the current formulation predicts significant lateral deviations for $R\omega_x/u$ values similar to the reported $R\omega_y/u$ values in planar collisions [14,26]. This is treated as an appendix (Appendix A2).

These factors could contribute to explain the relatively large dispersion in experimental data obtained in the determination of normal coefficients of restitution using the head-on impact of two aligned pendulums of equal length [46], a case of central impact without initial spin. This can be described using the IFR formalism as a head-on impact in the x-direction taking $\omega_x = 0$, $\omega_y = 0$, $\omega_z = 0$, $u_y = 0$, $u_z = 0$. Minute variations in the orientation of the oscillation plane and/or the length of the target pendulum and/or the acquisition of some initial spin during its 'fly' due to torsion effects would produce fluctuations in the impact parameters resulting in data dispersion.

Conjointly considered, all these results suggest that the variation of the tangential coefficient of restitution with the impact angle in the FR model can be seen as 'apparent': in all cases, the experimental data can satisfactorily be reproduced using the 'constant' tangential restitution coefficient defined in the IFR closure. The use of 'constant' coefficients of friction and restitution obviously facilitates the normalization of materials in, for instance, physics of sports. It is pertinent to underline, however, that the coefficients of friction and restitution vary, strictly, with the incoming velocity [6,16,18,30–36] so that the IFR closure (as the FR formulations treated here) is of application within the 'ordinary' range of experimental conditions involving moderate velocities and negligible viscous or adhesive effects.

4. Conclusions

The presented formulation of impact events, based on the independence of friction and restitution mechanisms, provides single expressions for the post-collision linear and angular velocities as functions of the pre-collision velocities and the coefficients of restitution (normal and tangential) and friction for both the stick and sliding regimes of impact. This IFR modeling uses a unique set of 'constant' coefficients of restitution (normal and tangential) and friction, thus avoiding the abrupt variation of the coefficient of tangential restitution with the impact angle appearing in conventional FR modeling.

Additionally, several experimental results considered as anomalous in literature can be interpreted as 'ordinary', in the proposed formulation, and appearing as the result, ultimately, of the coexistence of independent tangential restitution and friction effects. In spite of its simplicity, this phenomenological modeling could be of interest in the fields of fluids, granular matter, physics of sports, etc. where operative descriptions of the mechanics of collisions apply.

Credit author statement

The manuscript has been prepared and written by its unique autor, Antonio Doménech-Carbó.

Declaration of Competing Interest

The author declares no competing interest.

Data availability

Data will be made available on request.

Acknowledgments

Financial support from the Spanish R+D+I Project PID2020-113022GB-I00 supported by MCIN/AEI/10.13039/501100011033 is acknowledged.

Appendix A.1. Expressions for the postimpact linear and velocities predicted by the FR and IFR models in the case of planar collisions of a homogeneous sphere on a massive half-space

FR model, planar impact ($\omega_x = 0$):

$$v_z = e_n u cos\gamma \tag{A1.1}$$

$$\text{Sticking regime} : v_x = usin\gamma - \frac{2}{7}(1+\beta)\left(usin\gamma + R\omega_y\right) \tag{A1.2}$$

$$\text{Sliding regime} : v_x = usin\gamma - \mu(1+e_n)ucos\gamma \tag{A1.3}$$

$$\text{Sticking regime} : R\Omega_y = R\omega_y - \frac{5}{7}(1+\beta)\left(usin\gamma + R\omega_y\right) \tag{A1.4}$$

$$\text{Sliding regime} : R\Omega_y = R\omega_y - \frac{5}{2}\mu(1+e_n)ucos\gamma \tag{A1.5}$$

Velocities of the contacting point will be,

$$\text{Sticking regime} : V_t = -\beta\left(usin\gamma + R\omega_y\right) \tag{A1.6}$$

$$\text{Sliding regime} : V_t = usin\gamma + R\omega_y - \frac{2}{7}\mu(1+e_n)ucos\gamma \tag{A1.7}$$

IFR model, impact with arbitrary initial spin. The following equations reduce to those for planar impact taking $\omega_x = 0$ or, equivalently, $\sigma = 90$ deg. For both sliding and sticking regimes Eq. (A1.1) applies.

Sliding regime:

$$v_x = usin\gamma - \frac{2}{7}(1+e_t)U_{xy}cos\sigma - \mu(1+e_n)ucos\gamma cos\sigma \tag{A1.8}$$

$$v_y = -\frac{2}{7}(1+e_t)U_{xy}sin\sigma - \mu(1+e_n)ucos\gamma sin\sigma \tag{A1.9}$$

$$R\Omega_y = R\omega_y - \frac{5}{7}(1+e_t)U_{xy}cos\sigma - \frac{5}{2}\mu(1+e_n)ucos\gamma cos\sigma \tag{A1.10}$$

$$R\Omega_x = R\omega_x - \frac{5}{7}(1+e_t)U_{xy}sin\sigma - \frac{5}{2}\mu(1+e_n)ucos\gamma sin\sigma \tag{A1.11}$$

$$V_x = usin\gamma + R\omega_y - (1+e_t)U_{xy}cos\sigma - \frac{7}{2}\mu(1+e_n)ucos\gamma cos\sigma \tag{A1.12}$$

$$V_y = R\omega_x - (1+e_t)U_{xy}sin\sigma - \frac{7}{2}\mu(1+e_n)ucos\gamma sin\sigma \tag{A1.13}$$

Sticking regime:

$$v_x = usin\gamma - \left[\frac{2}{5} + \frac{2}{7}(1+e_t)\right]U_{xy}cos\sigma \tag{A1.14}$$

$$v_y = -\left[\frac{2}{5} + \frac{2}{7}(1+e_t)\right]U_{xy}sin\sigma \tag{A1.15}$$

$$R\Omega_y = R\omega_y - \left[1 + \frac{5}{7}(1+e_t)\right]U_{xy}cos\sigma \tag{A1.16}$$

$$R\Omega_x = R\omega_x - \frac{5}{7}(1+e_t)U_{xy}sin\sigma - \frac{5}{2}\mu(1+e_n)ucos\gamma sin\sigma \tag{A1.17}$$

$$V_x = usin\gamma + R\omega_y - (1+e_t)U_{xy}cos\sigma - \frac{7}{2}\mu(1+e_n)ucos\gamma cos\sigma \tag{A1.18}$$

$$V_y = R\omega_x - \left[\frac{7}{5} + (1+e_t)\right]U_{xy}sin\sigma \tag{A1.19}$$

For the limiting case in which $e_n = 0$, the z-component of the center of mass velocity becomes zero and the sphere moves after the impact over the massive plane. This mean $\delta = 90$ deg. but all other linear (and angular) velocity components do not cancel. The center of mass velocities will be, in the case of impact in sticking regime will be given by Eqs. (A1.14) and (A1.15) while in sliding regime, Eqs. (A1.8) and (A1.9) reduce to,

$$v_x = usin\gamma - \frac{2}{7}(1+e_t)U_{xy}cos\sigma - \mu ucos\gamma cos\sigma \tag{A1.20}$$

$$v_y = -\frac{2}{7}(1+e_t)U_{xy}sin\sigma - \mu ucos\gamma sin\sigma \quad \text{(A1.21)}$$

respectively. In the most drastic case, $e_n = 0$, $e_t = 0$, and the center of mass velocities before the impact in sticking regime will be,

$$v_x = usin\gamma - U_{xy}cos\sigma \quad \text{(A1.22)}$$

$$v_y = -U_{xy}sin\sigma \quad \text{(A1.23)}$$

In turn, the corresponding equations in sliding regime will be,

$$v_x = usin\gamma - \frac{2}{7}U_{xy}cos\sigma - \mu ucos\gamma cos\sigma \quad \text{(A1.24)}$$

$$v_y = -\frac{2}{7}U_{xy}sin\sigma - \mu ucos\gamma sin\sigma \quad \text{(A1.25)}$$

Appendix A2:

The IFR model presented here predicts significant lateral deviations of the sphere when it is projected with initial 'lateral' spin; i.e., when $\omega_x \neq 0$. This effect is particularly intense for small incidence angles, as can be seen in Fig. A1a. Here, the theoretically predicted variation of the lateral rebound angle λ with the incidence angle γ calculated from Eqs. (18), (19), (34), (35) taking $e_n = 0.90$, $e_t = -0.90$, $\mu = 0.15$, $\omega_y = 0$, and taking $R\omega_x/u = 0.30$, a value within the range of experimental $R\omega_y/u$ values reported in literature (between 0.2 and 0.8, see [14,26]). The influence of the value of the rotation rate can be seen in Fig. A1b when shows the variation of λ with the $R\omega_x/u$ ratio for rebounds also without forward/backward initial rotation ($\omega_y = 0$) when the impact angle is of $\gamma = 45$ deg. using the same values of the coefficients of friction and restitution.

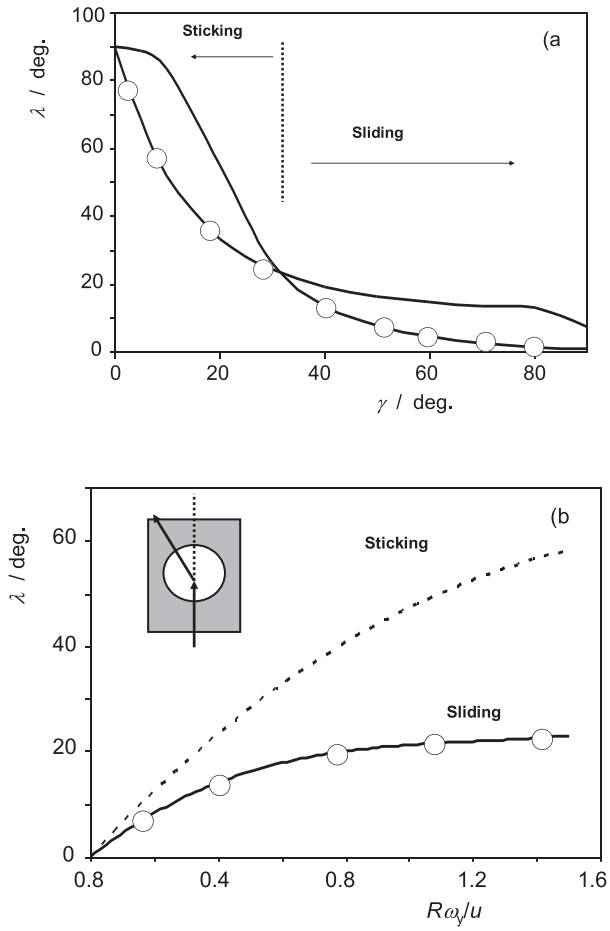

Fig. A2.1. Theoretical variation of the lateral rebound angle λ in the *xy* plane with: a) the incidence angle γ, and b) the $R\omega_x/u$ ratio calculated from Eqs. (18), (19), (34), (35) taking $e_n = 0.90$, $e_t = -0.90$, $\mu = 0.15$ when the impact takes place without forward/backward rotation ($\omega_y = 0$). a) Fixed value of $R\omega_x/u = 0.30$; b) fixed impact angle of $\gamma = 45$ deg. The circles represent idealized experimental data. Inset: zenithal view of the impact event.

References

[1] O.R. Walton, Numerical simulation of inelastic, frictional particle-particle interactions, in: M.C. Rocco (Ed.), Particulate Two-Phase Flow, Butterwort-Heinemann, Stonehem, 1993, pp. 884–911.
[2] N. Maw, J.R. Barber, J.N. Fawcett, The rebound of elastic bodies in oblique impact, Mech. Res. Commun. 4 (1977) 17–22.
[3] N. Maw, J.R. Barber, J.N. Fawcett, The oblique impact of elastic spheres, Wear 38 (1976) 101–114.
[4] R.M. Brach, Mechanical Impact Dynamics, John Wiley, New York, 2007.
[5] W.J. Stronge, Impact Mechanics, Cambridge Univ. Press, New York, 2000.
[6] P.F. Dunn, R.M. Brach, M.J. Caylor, Experiments on the low-velocity impact of microspheres with planar surfaces, Aerosol Sci. Technol. 23 (1995) 80–95.
[7] A. Lorenz, C. Tuozzolo, M.Y. Louge, Measurement of impact properties of small, nearly spherical particles, Exp. Mech. 37 (1997) 292–298.
[8] J. Calsamiglia, S.W. Kennedy, A. Chatterjee, A.L. Ruina, J.T. Jenkins, Anomalous frictional behavior in collisions of thin disks, ASME J. Appl. Mech. 66 (1999) 146–152.
[9] D.A. Gorham, A.H. Kharaz, The measurement of particle rebound characteristics, Powder Technol. 112 (2000) 193–202.
[10] X. Li, P.F. Dunn, R.M. Brach, Experimental and numerical studies of microsphere oblique impact with planar surfaces, J. Aerosol Sci. 31 (2000) 583–594.
[11] A.H. Kharaz, D.A. Gorham, A.D. Salman, An experimental study of the elastic rebound of spheres, Powder Technol. 120 (2001) 281–291.
[12] M.Y. Louge, M.E. Adams, Anomalous behavior of normal kinematic restitution in the oblique impacts of a hard sphere on an elasto-plastic plate, Phys. Rev. E 65 (2002), 021303.
[13] G.G. Joseph, M.L. Hunt, Oblique particle-wall collisions in a liquid, J. Fluid Mech. 510 (2004) 71–93.
[14] H. Dong, M.H. Moys, Experimental study of oblique impacts with initial spin, Powder Technol. 161 (2006) 22–31.
[15] O.V. Kim, P.F. Dunn, A microsphere-surface impact model for implementation in computational fluid dynamics, J. Aerosol Sci. 38 (2007) 532–549.
[16] R. Mourya, A. Chatterjee, Anomalous frictional behavior in collisions of thin disks revisited, ASME J. Appl. Mech. 75 (2008), 024501.
[17] C.Y. Wu, C. Thornton, L.-Y. Li, A semi-analytical model for oblique impact of elastoplastic spheres, Proc. Roy. Soc. A 465 (2009) 937–960.
[18] A. Le Quiniou, F. Rioual, P. Héritier, Y. Lapusta, Experimental study of the bouncing trajectory of a particle along a rotating wall, Phys. Fluids 21 (2009) 12–20.
[19] S. Antonyuk, S. Heinrich, J. Tomas, N.G. Deen, M.S. van Buijtenen, J.A.M. Kuipers, Energy absorption during compression and impact of dry elastic-plastic spherical granules, Granul. Matter 12 (2010) 15–47.
[20] P. Mueller, S. Antonyuk, M. Stasiak, J. Tomas, S. Heinrich, The normal and oblique impact of three types of wet granules, Granul. Matter 13 (2011) 455–463.
[21] C.J. Reagle, J.M. Delimont, W.F. Ng, et al., Measuring the coefficient of restitution of high speed microparticle impacts using a PTV and CFD hybrid technique, Meas. Sci. Technol. 24 (2013), 105303.
[22] K. Yu, D. Tafti, Impact model for micrometer-sized sand particles, Powder Technol. 294 (2016) 11–21.
[23] B. Buck, Y. Tang, S. Heinrich, N.G. Deen, J.A.M. Kuipers, Collision dynamics of wet solids: rebound and rotation, Powder Technol. 316 (2017) 218–224.
[24] J. Xie, M. Dong, S. Li, Y. Mei, Y. Shang, An experimental study of fly ash particle oblique impact with stainless surfaces, J. Aerosol Sci. 123 (2018) 27–38.
[25] V. Tomar, M. Bose, Anomalies in normal and oblique collision properties of spherical particles, Powder Technol. 325 (2018) 669–677.
[26] R. Cross, Oblique impact of a steel ball, Powder Technol. 351 (2019) 282–290.
[27] K. Hashemnia, O. Askari, Experimental and finite element analysis of oblique impacts with different initial spins, Mech. Res. Commun. 99 (2019) 68–72.
[28] J. Wang, M. Zhang, L. Feng, H. Yang, Y. Wu, G. Yue, The behaviors of particle-wall collision for non-spherical particles: experimental investigation, Powder Technol. 363 (2020) 187–194.
[29] S. Zhang, N. Gui, X. Huang, L. Ge, XT. Yang, J. Tu, S. Jiang, Verifying the tangential and normal restitution coefficients for double-sphere particles, Powder Technol. (2020) 419–427.
[30] N.V. Brilliantov, V. Spahn, J.-M. Hertzsch, T. Pöschel, Model for collisions in granular gases, Phys. Rev. E 53 (1996) 5382–5392.
[31] C. Thornton, Z. Ning, A theoretical model for the stick/bounce behaviour of adhesive, elastic-plastic spheres, Powder Technol. 99 (1998) 154–162.
[32] L. Vu-Quoc, X. Zhang, An elasto-plastic contact force-displacement model in the normal direction: displacement-driven version, Proc. Roy. Soc. London A 455 (1999) 4013–4044.
[33] C. Thornton, S.J. Cummins, P.W. Cleary, An investigation of the comparative behaviour of alternative contact force models during inelastic collisions, Powder Technol. 210 (2011) 189–197.
[34] C. Thornton, S.J. Cummins, P.W. Cleary, An investigation of the comparative behaviour of alternative contact force models during inelastic collisions, Powder Technol. 233 (2013) 30–46.
[35] S. Schwager, V. Becker, V.T. Pöschel, Coefficient of tangential restitution for visocoelastic spheres, Eur. Phys. J. E 27 (2008) 107–114.
[36] S. Luding, Cohesive, frictional powders: contact models for tension, Granul. Matter 10 (2008) 235–246.
[37] C.C. Lai, A.N. Huang, C.Y. Chen, W.Y. Hsu, J.P.K. Seville, H.P. Kuo, Modification of the spherical particle spring-damping contact model from contact velocity dependent restitution coefficients, Powder Technol. 401 (2022), 117294.
[38] A. Doménech-Carbó, Analysis of oblique rebound using a redefinition of the coefficient of tangential restitution coefficient, Mech. Res. Commun. 54 (2013) 35–40.
[39] A. Doménech-Carbó, On the tangential restitution problem: independent friction-restitution modeling, Granul. Matter 16 (2014) 573–582. See erratum in Granular Matter, 16 (2014) 945.
[40] A. Doménech-Carbó, On the independence of friction and restitution: an operational approach, Granul. Matter 18 (2016) 9–23.
[41] A. Doménech-Carbó, Analysis of rolling friction effects on oblique rebound by redefining tangential restitution and friction, Phys. Fluids 31 (2019), 043302.
[42] A. Doménech-Carbó, C. Doménech-Casasús, Analysis of microsphere oblique impact with planar surfaces based on the independent friction-restitution approach, J. Aerosol Sci. 140 (2020), 105482.
[43] A. Doménech-Carbó, Independent friction-restitution approach to analyze anomalies in normal kinematic restitution in oblique impact, Mech. Res. Commun. 113 (2021), 103699.
[44] R.M. Brach, Friction, restitution, and energy loss in planar collisions, ASME J. Appl. Mech. 51 (1984) 164–170.
[45] J.E. Higham, P. Shepley, M. Shahnam, Measuring the coefficient of restitution for all six degrees of freedom, Granul. Matter 21 (2019) 15.
[46] J. Hlosta, D. Žurovec, J. Rozbroj, A. Ramírez-Gómez, J. Nečas, J. Zegjulka, Experimental determination of particle–particle restitution coefficient via double pendulum method, Chem. Eng. Res. Design 135 (2018) 222–233.